Available online at www.sciencedirect.com
SCIENCE DIRECT
Journal of Power Sources 148 (2005) 90–94
JOURNAL OF POWER SOURCES
www.elsevier.com/locate/jpowsour

Improving the electrochemical behavior of $LiCoO_2$ electrode by mixed Zr–Mg doping

H.Y. Xu, S. Xie, C.P. Zhang, C.H. Chen *

Department of Materials Science and Engineering, University of Science and Technology of China, Anhui Hefei 230026, PR China

Received 14 July 2004; received in revised form 31 January 2005; accepted 1 February 2005
Available online 2 April 2005

Abstract

A new class of $LiCo_{1-x}Zr_{x/2}Mg_{x/2}O_2$ ($x = 0$, 0.02, 0.06, 0.10, 0.20) materials has been synthesized using a solution–combustion method with mixed acetates/nitrates as the starting materials. The structure of the synthesized oxides was analyzed using X-ray diffraction (XRD). Iodometry titration was used to measure the oxidation state of cobalt. The electrochemical performance of $LiCo_{1-x}Zr_{x/2}Mg_{x/2}O_2$ electrodes was analyzed using cyclic voltammetry (CV), electrochemical impedance spectroscopy (EIS), and galvanostatic charge–discharge cycling studies in the voltage range 2.7–4.2 V (versus Li metal). It is found that the maximum doping level (x) is around 0.06, above which Li_2MgZrO_4 is formed as an impurity phase. The use of combined Zr–Mg doping has resulted in the decrease of the electrode impedance and increase of the specific capacity and the stability of 3.6 V plateau efficiency.

Keywords: Lithium cobalt oxide; Doping; Plateau efficiency; Rechargeable battery

1. Introduction

Lithium ion rechargeable batteries not only have important applications in portable electronics but also are potential long-term candidates for powering emission-free vehicles. $LiCoO_2$, $LiNiO_2$, and $LiMn_2O_4$ are the most attractive cathode (positive electrode) materials. Among these materials, $LiCoO_2$ has the best performance and is the most widely used in commercial lithium ion batteries. It is well established that the practical capacity of $LiCoO_2$ is limited to about 140 mAh g^{-1}, i.e. around half of its theoretical capacity (273 mAh g^{-1}) because when x in Li_xCoO_2 is less than 0.5, the layered structure collapsed easily [1–3]. On the other hand, the capacity fade of a cell with $LiCoO_2$ as the cathode is largely related to the surface reaction between the oxidizing Co^{4+} in the charged state and the electrolyte solvent [4]. Therefore, bulk doping and surface modification are two natural strategies to improve the electrochemical performance of $LiCoO_2$ electrode. In fact, they are also effective for other positive electrode materials such as $LiNiO_2$ and $LiMn_2O_4$.

Recently, attempts for the $LiCoO_2$ improvement by means of doping or coating with some inactive metal oxides have shown positive results in increasing the capacity and enhancing the stability of the $LiCoO_2$ electrodes. These metal oxides include MgO [5,6], B_2O_3 [7], SiO_2 [8], Al_2O_3 [5,8,9], and ZrO_2 [8,10]. This kind of modification leads to either better capacity retention through suppressing the surface reaction on the $LiCoO_2$ particles or higher accessible specific capacity with a higher upper limit of the intercalation voltage through forming stronger M–O bonding to stabilize the layered structure at its highly delithiated state. Another by-product of such a modification is that the material cost of the modified $LiCoO_2$ production may be reduced because cobalt is a relatively expensive metal. As for the Mg or Zr doping, the exact mechanism is not very clear at this moment. Recently, Kim et al. reported that both Mg and Zr doping lead to the increase of $LiCoO_2$ lattice parameters a and c owing to the larger ion sizes of Mg^{2+} or Zr^{4+} compared to that of Co^{3+} [11]. As a result,

* Corresponding author. Tel.: +86 551 3602938; fax: +86 551 3602940.
E-mail address: cchchen@ustc.edu.cn (C.H. Chen).

0378-7753/$ – see front matter © 2005 Published by Elsevier B.V.
doi:10.1016/j.jpowsour.2005.02.005

such a lattice doping improves the cycleability of $LiCoO_2$ in the wide voltage window between 3.0 and 4.5 V. Nevertheless, they only investigated the effect of single-element doping (i.e. either Mg or Zr doping). They think that after doping, the $Mg^{2+}$and Zr^{4+} ions moved to the inter-slab space along with Co^{4+} ions during the de-intercalation of Li^+ ions over 4.2 V and they locate at the position of Li assisting the movement of Li^+ ions by preventing the vacancy ordering. Thus, both Mg and Zr doping can make the $LiCoO_2$ structure stable. However, the specific capacity has no increase when charged to 4.2 V. Considering the fact of tri-valence of Co in $LiCoO_2$, we investigated the effect of mixed doping with equal amount of divalent Mg and tetravalent Zr in the $LiCoO_2$ in this study. Hopefully, like the single-element doping, the lattice parameters *a* and *c* increase as well so that a more open lattice structure is derived and the lithium ion can intercalate or de-intercalate more easily. By this way, the cell impedance can be decreased accordingly. Some interesting results have been obtained.

2. Experimental

2.1. Synthesis of $LiCo_{1-x}Zr_{x/2}Mg_{x/2}O_2$ powders

Lithium nitrate ($LiNO_3$), lithium acetate ($Li(CH_3COOH)\cdot 2H_2O$), cobalt acetate ($Co(CH_3COOH)_2\cdot 4H_2O$), zirconium nitrate ($Zr(NO_3)_4\cdot 5H_2O$) and magnesium nitrate ($Mg(NO_3)_2\cdot 6H_2O$) were used as the starting materials. The molar ratio of nitrate group (NO_3^-) to acetate group (CH_3COOH^-) was controlled to be about 1:2. They were dissolved in deionized water and stirred thoroughly to make a clear solution, which was then heated at 150 °C for about 4 h to form a xerogel. This xerogel was heated to 300 °C so that a self-combustion of the solution took place and a very fine powder was obtained. It was ground mildly at ambient temperature and then sintered at 850 °C for 12 h. The sintered powder was well ground and used for physical and electrochemical investigations. Note that a small excess of lithium was used (the molar ratio Li/(Co + Zr + Mg) = 1.05) in order to compensate the evaporation loss of lithium.

2.2. Structural and composition analyses

The crystal structure of the powders was analyzed using X-ray diffraction (Rigaku D/Max-rA, Cu $K\alpha_1$ radiation). The scanned range was from 10° to 80° (2θ). The average oxidation state of cobalt in the doped $LiCoO_2$ samples was determined by the iodometry titration. In this analysis, $LiCoO_2$ was first dissolved in a dilute hydrochloric acid solution. The reduction of Co^{4+} and Co^{3+} to Co^{2+} was achieved by adding I^- into the solution, forming I_3^-. Back titration for the resulting I_3^- was carried out by a $Na_2S_2O_3$ solution with a predetermined concentration. Thus, the average oxidation state of cobalt can be calculated.

2.3. Electrode preparation and electrochemical measurements

The electrode laminate for the electrochemical testing was prepared by casting a slurry consisting of active material powders (84 wt.%), acetylene black (8 wt.%), and poly(vinylidene fluoride) (PVDF) (8 wt.%) dispersed in 1-methyl-2-pyrrolidinone (NMP) onto an aluminum foil. The laminates were then dried at 70 °C for 2 h.

The $LiCo_{1-x}Zr_{x/2}Mg_{x/2}O_2$/Li coin-cells (2032 size) were made with 1 M $LiPF_6$ in ethylene carbonate (EC):diethyl carbonate (DEC) (1:1, w/w) as the electrolyte. The cells were tested on a multi-channel battery cycler (Shenzhen Neware Co. Ltd.) and subjected to charge–discharge cycles at 0.2 mA cm^{-2} and approximately 1 C-rate, respectively, between 2.7 and 4.2 V (versus Li metal). Cyclic voltammograms of these cells were measured on a CHI 604A Electrochemical Workstation from 3.0 to 4.5 V at a scanning rate of 0.2 mV s^{-1}. In addition, ac impedance spectroscopy was also performed on CHI 604A in the frequency range from 0.001 to 100 kHz.

The internal resistance of the cells was also measured by a current interruption technique. This was done by applying intermittently a zero current pulse through the process of charge and recording the voltage change before and after interruption. Thus, the dc resistance of a cell (R_{dc}) at a certain state-of-charge (SOC) can be calculated as $R_{dc} = \Delta U/\Delta I$.

3. Results and discussion

3.1. Structure analysis

Fig. 1 shows the XRD patterns of the $LiCo_{1-x}Zr_{x/2}Mg_{x/2}O_2$ powders. It can be seen that pure phases of α-$NaFeO_2$ layered structure were obtained when $0 \le x \le 0.06$. When $x \ge 0.1$ there appears an impurity phase that is identified to be tetragonal Li_2ZrMgO_4 [12]. Therefore, the maximum doping level (*x*) seems to be between 0.06 and 0.1.

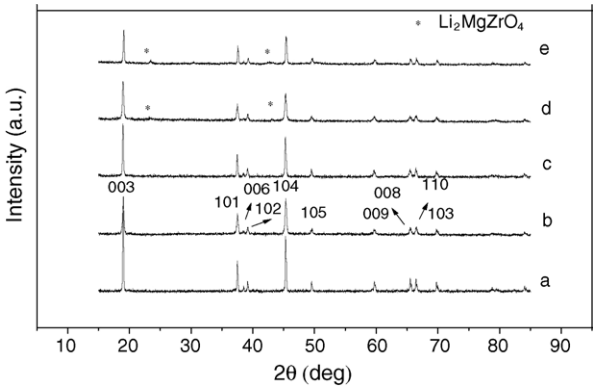

Fig. 1. X-ray diffraction patterns of $LiCo_{1-x}Zr_{x/2}Mg_{x/2}O_2$: (a) $x = 0$; (b) $x = 0.02$; (c) $x = 0.06$; (d) $x = 0.1$; (e) $x = 0.2$. The peaks indicated by star are from the diffraction of Li_2MgZrO_4.

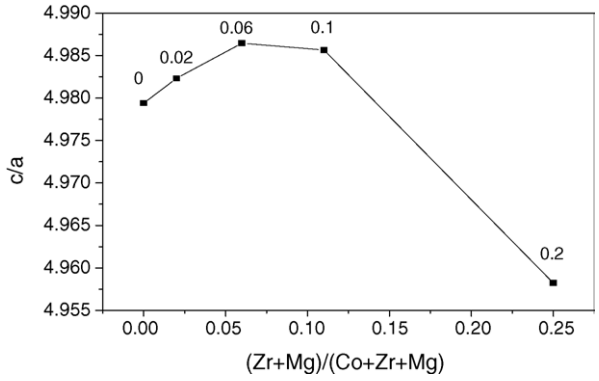

Fig. 2. The lattice parameter c/a ratio as a function of x in $LiCo_{1-x}Zr_{x/2}Mg_{x/2}O_2$ powder samples.

Assuming the maximum level as 0.06, according to the mass balance, following equations for the doped composition can be written:

$$\text{“}LiCo_{1-x}Zr_{x/2}Mg_{x/2}O_2\text{”} \rightarrow LiCo_{1-x}Zr_{x/2}Mg_{x/2}O_2 \quad (x \leq 0.06) \tag{1}$$

$$\text{“}LiCo_{1-x}Zr_{x/2}Mg_{x/2}O_2\text{”} \rightarrow (1.06-x)LiCo_{0.94}Zr_{0.03}Mg_{0.03}O_2 + (x/2-0.03)Li_2MgZrO_4 \quad (x > 0.06) \tag{2}$$

Since well-defined peak doublets (0 0 6, 0 1 2) and (0 1 8, 1 1 0) appear in all of these patterns, it is an indication of the stabilization of the two-dimensional structure and an ordered distribution of lithium and cobalt ions in the lattice. The lattice constants a and c can be calculated by the formula: $d_{hkl} = 1/[4(h^2+hk+k^2)/3a^2 + l^2/c^2]^{1/2}$. It is found that, similar to the single-element doping [11], the a and c generally increases from $a = 2.8115$ Å and $c = 13.9995$ Å for $LiCoO_2$ to $a = 2.8125$ Å and $c = 14.0238$ Å for $LiCo_{0.94}Zr_{0.03}Mg_{0.03}O_2$. On the other hand, an approximate indication of cation disorder can be discerned from the lattice parameter ratio c/a [13]. As seen from Fig. 2, the c/a ratio increases with x when $x < 0.06$, reaches a plateau in the region of $0.06 \leq x \leq 0.1$, and then decreases abruptly. This suggests increased layered characteristics, or that the lattice expands preferentially in the c-direction in the region of $0 \leq x \leq 0.06$. This kind of structure alternation is in favor of Li ion inserting and extracting. Since Mg^{2+} has been found to have only a small effect on the crystal lattice of $LiCoO_2$, especially at higher substituent levels [14], the lattice change here should be mainly caused by the Zr doping.

The iodometry titration results show that the Co oxidation states in $LiCo_{1-x}Zr_{x/2}Mg_{x/2}O_2$ ($x = 0$, 0.02, 0.06, 0.10) are 2.94, 2.94, 2.95, 2.96, respectively. Thus, no obvious change in the Co oxidation state is detected. If only Mg is doped in $LiCoO_2$, the Co oxidation states would increase compared with the non-doped $LiCoO_2$. On the contrary, Zr doping in $LiCoO_2$ would lead to the decrease of Co oxidation state.

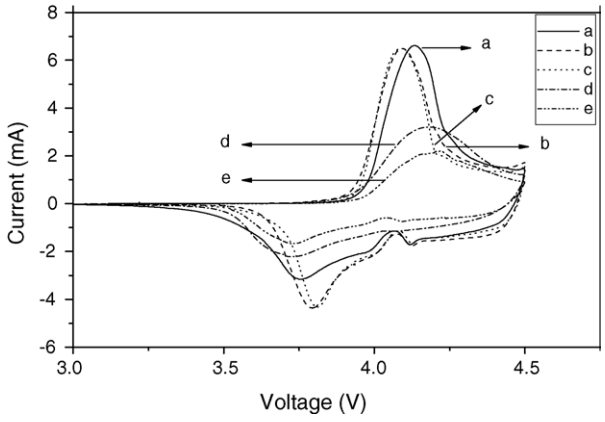

Fig. 3. Cyclic voltammograms of $LiCo_{1-x}Zr_{x/2}Mg_{x/2}O_2$/Li cells with 1 M $LiPF_6$/EC + DEC as the electrolyte. Scan rate was 0.02 mV s^{-1}: (a) $x = 0$; (b) $x = 0.02$; (c) $x = 0.06$; (d) $x = 0.1$; (e) $x = 0.2$.

Therefore, we believe that equal amount of Zr and Mg have been doped in the $LiCoO_2$ lattice in these samples.

3.2. Electrochemical characterization

Cyclic voltammograms (CV) of $LiCo_{1-x}Zr_{x/2}Mg_{x/2}O_2$/Li cells in the second cycle are given in Fig. 3. They show typical CV curves of high temperature (HT) phase of $LiCoO_2$, with a main intercalation/de-intercalation peak around 3.9 V and two small peaks above this potential [15–17]. It is noticed that the peak separation becomes narrower with x when $x \leq 0.06$ and then becomes wider with x when $x \geq 0.06$. Meanwhile, the peak intensity increases first and decreases then with x. This kind of change should be related to the polarization effect due to the variation of cell impedance. Obviously, a small amount of Zr–Mg doping results in easier lithium insertion and extraction, which is correspondent with the changes of c/a value (Fig. 2).

The capacity change with the cycle number for the $LiCo_{1-x}Zr_{x/2}Mg_{x/2}O_2$/Li cells is presented in Fig. 4.

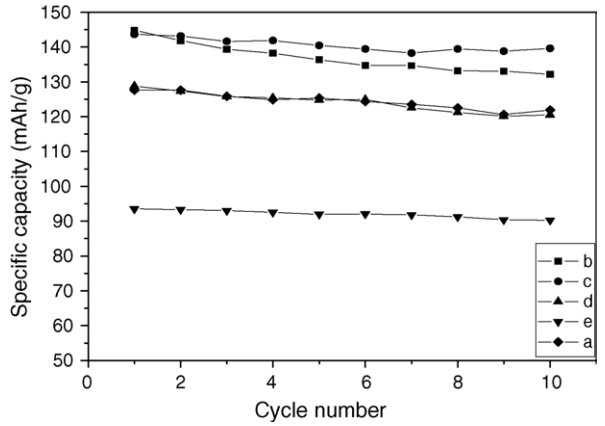

Fig. 4. Small current discharge capacity $LiCo_{1-x}Zr_{x/2}Mg_{x/2}O_2$/Li cells at the current density of 0.2 mA cm^{-2}: (a) $x = 0$; (b) $x = 0.02$; (c) $x = 0.06$; (d) $x = 0.1$; (e) $x = 0.2$.

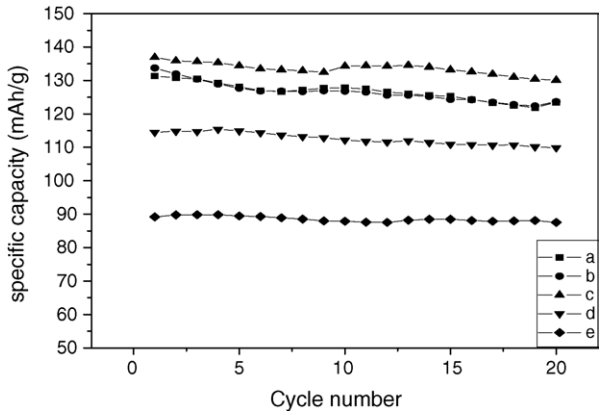

Fig. 5. 1 C-rate discharge capacity $LiCo_{1-x}Zr_{x/2}Mg_{x/2}O_2$/Li cells: (a) $x = 0$; (b) $x = 0.02$; (c) $x = 0.06$; (d) $x = 0.1$; (e) $x = 0.2$.

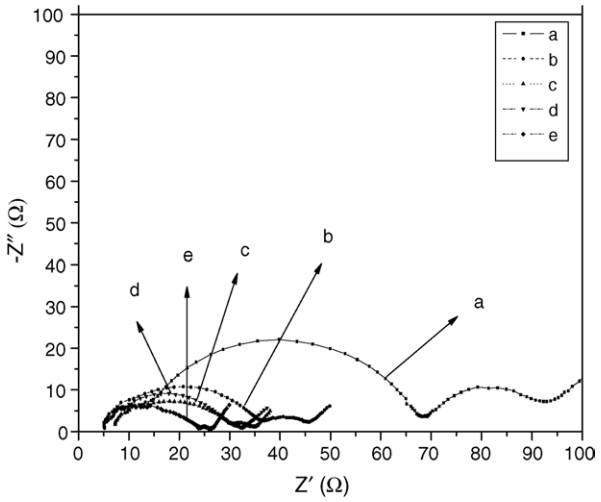

Fig. 6. Electrochemical impedance spectra of $LiCo_{1-x}Zr_{x/2}Mg_{x/2}O_2$/Li cells at 4.2 V of the open circuit voltage: (a) $x = 0$; (b) $x = 0.02$; (c) $x = 0.06$; (d) $x = 0.1$; (e) $x = 0.2$.

The first discharge capacities of $LiCo_{0.98}Zr_{0.01}Mg_{0.01}O_2$ and $LiCo_{0.94}Zr_{0.03}Mg_{0.03}O_2$ are 145 and 144 mAh g^{-1}, respectively. In subsequent cycles, $LiCo_{0.94}Zr_{0.03}Mg_{0.03}O_2$ remains to possess the highest capacity of all samples and 96% of the initial capacity is retained, while the non-doped $LiCoO_2$ only has 128 mAh g^{-1} initial capacity that is approximately equal to the capacity of $LiCo_{0.90}Zr_{0.05}Mg_{0.05}O_2$. Similar sequence of capacity values is also found for the 1 C-rate cycling (Fig. 5); $LiCo_{0.94}Zr_{0.03}Mg_{0.03}O_2$ still shows the highest capacity. This trend is also found in the cases of Ti-doped $LiCoO_2$ [18]. The maximum Ti doping level to obtain pure rock-salt phase with better electrochemical property is about 0.01. After $x \geq 0.05$, there appears also an impurity phase. Therefore, a small amount of aliovalent dopant is favorable to improve the performance of $LiCoO_2$. Furthermore, the specific capacity obtained with the Mg–Zr mixed doping with the cut-off voltage at 4.2 V is nearly the same as that for the best Mg or Zr single-element-doped $LiCoO_2$ with the cut-off voltage at 4.3 V. Therefore, the mixed doping apparently results in higher capacity compared to the case of Mg or Zr single-element doping due probably to its decreased impedance (see below).

The ac impedance spectra of the $LiCo_{1-x}Zr_{x/2}Mg_{x/2}O_2$/Li cells at their fully charged state (about 4.2 V) after 20 cycles are shown in Fig 6. Obviously, as a result of Zr–Mg doping, the cell impedance decreases substantially. Considering the fact that all these cells use the same Li electrode and electrolyte, the difference should be dominantly contributed from the cathode ($LiCo_{1-x}Zr_{x/2}Mg_{x/2}O_2$ side). Assuming the equivalent circuit of this cathode impedance is similar to the case of $LiNi_{0.8}Co_{0.2}O_2$/Li cells [19], the high frequency semicircle and the intermediate frequency semicircle on these spectra are associated with the surface film resistance (R_{sf}) and charge transfer resistance (R_{ct}) on the cathode side, respectively. Thus, it can be seen from Fig. 6 that both R_{sf} and R_{ct} decrease with increasing the Zr–Mg doping level. The minimum impedance corresponds to $x = 0.2$. It appears that the existence of Li_2MgZrO_4 helps to reduce R_{sf}. This result suggests that Li_2MgZrO_4 could be a good lithium ion conductor. The dc resistance measurement also indicates the same relationship of cell impedance versus doping level holds roughly for other depth-of-discharge (DOD) (Fig. 7). On the other hand, according to the reaction (2), the amount of active material is less than the nominal value when $x > 0.06$. Thus, the trade-off of the cell impedance and the amount of active material leads to achieve the highest specific capacity when $x = 0.06$, as shown in Figs. 4 and 5.

As plateau efficiency is a stricter control parameter than the capacity retention to evaluate the quality of electrode materials for lithium ion cells [20], we studied the 3.6 V plateau efficiency of $LiCo_{1-x}Zr_{x/2}Mg_{x/2}O_2$/Li cells. It can be seen from Fig. 8 that only pristine $LiCoO_2$ decreases rather rapidly with cycle number, while Zr–Mg-doped samples varies slightly during 20 cycles at the rate of 1 C discharge. This means that the Zr–Mg doping has improved the stability of the discharge plateau efficiency. Therefore, the

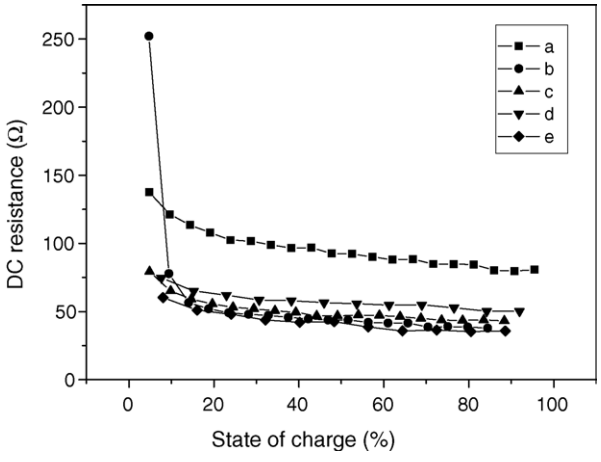

Fig. 7. The direct current resistance of $LiCo_{1-x}Zr_{x/2}Mg_{x/2}O_2$/Li cells as a function of state-of-charge: (a) $x = 0$; (b) $x = 0.02$; (c) $x = 0.06$; (d) $x = 0.1$; (e) $x = 0.2$.

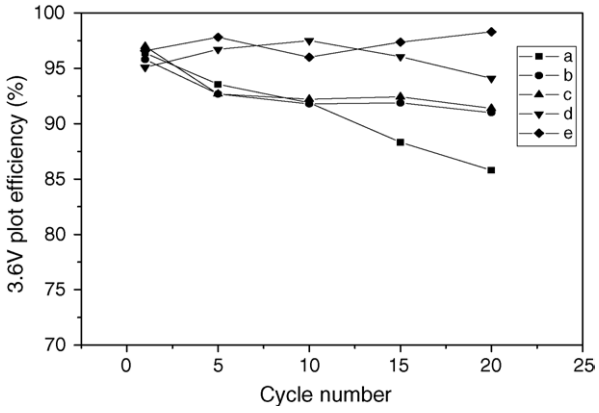

Fig. 8. The 3.6 V plateau efficiency of $LiCo_{1-x}Zr_{x/2}Mg_{x/2}O_2$/Li cells in the voltage range between 4.2 and 2.7 V at 1 C-rate discharge: (a) $x = 0$; (b) $x = 0.02$; (c) $x = 0.06$; (d) $x = 0.1$; (e) $x = 0.2$.

application of such doped electrodes has the potential to extend the cycle life of a practical lithium ion cell. The reason of this improvement must be related to the decreased impedance and stability of the doped electrodes.

4. Conclusions

$LiCo_{1-x}Zr_{x/2}Mg_{x/2}O_2$ ($0 \leq x \leq 0.2$) powders were prepared by a solution–combustion route. An impurity phase tetragonal Li_2ZrMgO_4 was identified when $x \geq 0.1$, therefore the maximum doping level is between 0.06 and 0.1. The optimal electrochemical performance of this doped $LiCoO_2$ system is obtained when $x = 0.06$. Both specific capacity and the stability of 3.6 V plateau efficiency are improved by the combined Zr–Mg doping. The fact that the cell impedance of $LiCo_{1-x}Zr_{x/2}Mg_{x/2}O_2$/Li samples decreases with x increase suggests that Li_2MgZrO_4 could be a good lithium ion conductor.

Acknowledgements

This study was supported by 100 Talents Program of Academia Sinica and National Science Foundation of China (grant nos. 50372064 and 20471057). We are also grateful to the China Education Ministry (SRFDP no. 2003035057).

References

[1] J.N. Reimers, J.R. Dahn, J. Electrochem. Soc. 139 (1992) 2091.
[2] M. Menetrier, I. Saadoune, S. Levasseur, C. Delmas, J. Mater. Chem. 9 (1999) 1135.
[3] S. Levasseur, M. Menetrier, C. Delmas, J. Power Sources 112 (2002) 419.
[4] G.G. Amatucci, J.M. Tarascon, L.C. Klein, Solid State Ionics 83 (1996) 167.
[5] Z.X. Wang, L.J. Liu, L.Q. Chen, X.J. Huang, Solid State Ionics 148 (2002) 335.
[6] H. Tukamoto, A.R. West, J. Electrochem. Soc. 144 (1997) 3164.
[7] R. Alcantara, P. Lavela, J.L. Tirado, R. Stoyanova, E. Zhecheva, J. Solid State Chem. 134 (1997) 265.
[8] Z.H. Chen, J.R. Dahn, Electrochem. Solid-State Lett. 6 (2003) 221.
[9] W.S. Yoon, K.K. Lee, K.B. Kim, Electrochem. Solid-State Lett. 4 (2001) 35.
[10] Z.H. Chen, J.R. Dahn, Electrochem. Solid-State Lett. 5 (2002) 213.
[11] H.S. Kim, T.K. Ko, B.K. Na, W.I. Cho, B.W. Chao, J. Power Sources 138 (2004) 232.
[12] JCPDF card no. 78-0198.
[13] S. Madhavi, G.V.S. Rao, B.V.R. Chowdari, S.F.Y. Li, J. Electrochem. Soc. 148 (2001) 1279.
[14] R. Thirunakaran, N. Kalaiselvi, P. Periasamy, N.G. Renganathan, Ionics 9 (2003) 388.
[15] C.J. Ohzuku, A. Ueda, J. Electrochem. Soc. 144 (1997) 2780.
[16] J.N. Reimers, J. Dahn, J. Electrochem. Soc. 139 (1992) 2091.
[17] T. Ohzuku, A. Veda, M. Nagayama, J. Electrochem. Soc. 141 (1994) 2972.
[18] S. Gopukumara, Y. Jeongb, K.B. Kim, Solid State Ionics 159 (2003) 223.
[19] C.H. Chen, J. Liu, K. Amine, J. Power Sources 96 (2001) 321.
[20] J. Zhang, Y.J. Xiang, Y. Yu, S. Xie, G.S. Jiang, C.H. Chen, J. Power Sources 132 (2004) 187.